ACS APPLIED MATERIALS & INTERFACES

Research Article

www.acsami.org

Triple Shape Memory Effect of Star-Shaped Polyurethane

Xifeng Yang, Lin Wang, Wenxi Wang, Hongmei Chen, Guang Yang, and Shaobing Zhou*

Key Laboratory of Advanced Technologies of Materials, Ministry of Education, School of Materials Science and Engineering, Southwest Jiaotong University, Chengdu 610031, P.R. China

Supporting Information

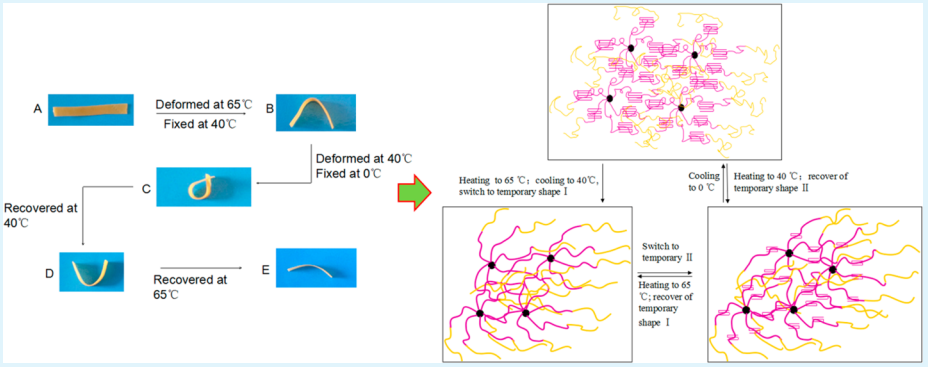

ABSTRACT: In this study, we synthesized one type of star-shaped polyurethane (SPU) with star-shaped poly(ε-caprolactone) (SPCL) containing different arm numbers as soft segment and 4,4′-diphenyl methane diisocyanate (MDI) as well as chain extender 1,4-butylene glycol (BDO) as hard segment. Proton nuclear magnetic resonance (^{1}H-NMR) confirmed the chemical structure of the material. Differential scanning calorimetry (DSC) and dynamic mechanical analysis (DMA) results indicated that both the melting temperature (T_m) and transition temperature (T_{trans}) of SPU decreased with the hard segment composition increase. X-ray diffraction (XRD) results demonstrated that the increase of the crystallinity of SPU following the raised arm numbers endowed a high shape fixity of six-arm star-shaped polyurethane (6S-PU) and a wide melting temperature range, which resulted in an excellent triple-shape memory effect of 6S-PU. The in vitro cytotoxicity assay evaluated with osteoblasts through Alamar blue assay demonstrates that this copolymer possessed good cytocompatibility. This material can be potentially used as a new smart material in the field of biomaterials.

KEYWORDS: *star-shaped polyurethane, wide melting range, biocompatibility, crystallinity, triple-shape memory effect*

INTRODUCTION

Shape memory polymers (SMPs) are a kind of smart materials that can be deformed into a temporary shape upon application of an external stimulus, typically heat. And this temporary shape can be removed almost completely at the situation in which stimulus is exerted on it again.[1,2] Many polymers, such as polyester,[3,4] poly(ether-ether-ketone),[5] polynorbornene,[6] cross-linked polyethylene (PE),[7] and polyurethane (PU),[8,9] had been reported that they can exhibit shape memory effect. Up to now, SMPs have been widely spread in numerous applications, for instance, biomedical,[10] information carriers,[11] spinning.[12] Especially in biomedical fields, contain the following applications, drug delivery,[13] implanting,[14,15] suture,[16] and wound healing[17,18] because of their unique properties, such as a wide range of shape memory temperature, high shape recover ratio, good process ability, and excellent biocompatibility.[19]

In the shape memory process of thermally induced shape memory polyurethanes (TSMPUs), polyether and polyester are often used as soft segment to fix temporary shape, whereas diisocyanate and chain extender are utilized as hard segment for shape recovery.[12,19] So far, TSMPUs usually were linear block copolymers consisting of switch segment for the fixation of the temporary shape and the hard segment for the recovery of permanent shape.[20,21] However, these linear TSMPUs cannot ensure cyclic thermal-mechanical analysis, and the retention and recovery properties of shape memory polymer will decrease after repeating for several times. In comparison with corresponding linear polymers, star-shaped polyurethane (SPU) has unique properties because of its well-defined branched structures, a large number of functional groups available in a small volume, controlled functionality, and composition.[22,23] Hence, some researchers have transferred their sights to the star-shaped polyurethane. For example, star-shaped inorganic polyhedral oligomeric silsesquioxane (POSS)-poly(ε-caprolactone) polyurethanes with POSS core as initiator exhibited remarkable shape cycles-averaged shape fixities and shape recoverabilities;[24] a three-arm star-shaped polymer that used the glycol initiating ε-caprolactone (ε-CL) obtained a switching temperature around body temperature.[25] Other

Received: January 8, 2014
Accepted: March 11, 2014
Published: March 11, 2014

   dx.doi.org/10.1021/am5001344 | ACS Appl. Mater. Interfaces 2014, 6, 6545−6554

Scheme 1. Synthesis of SPU

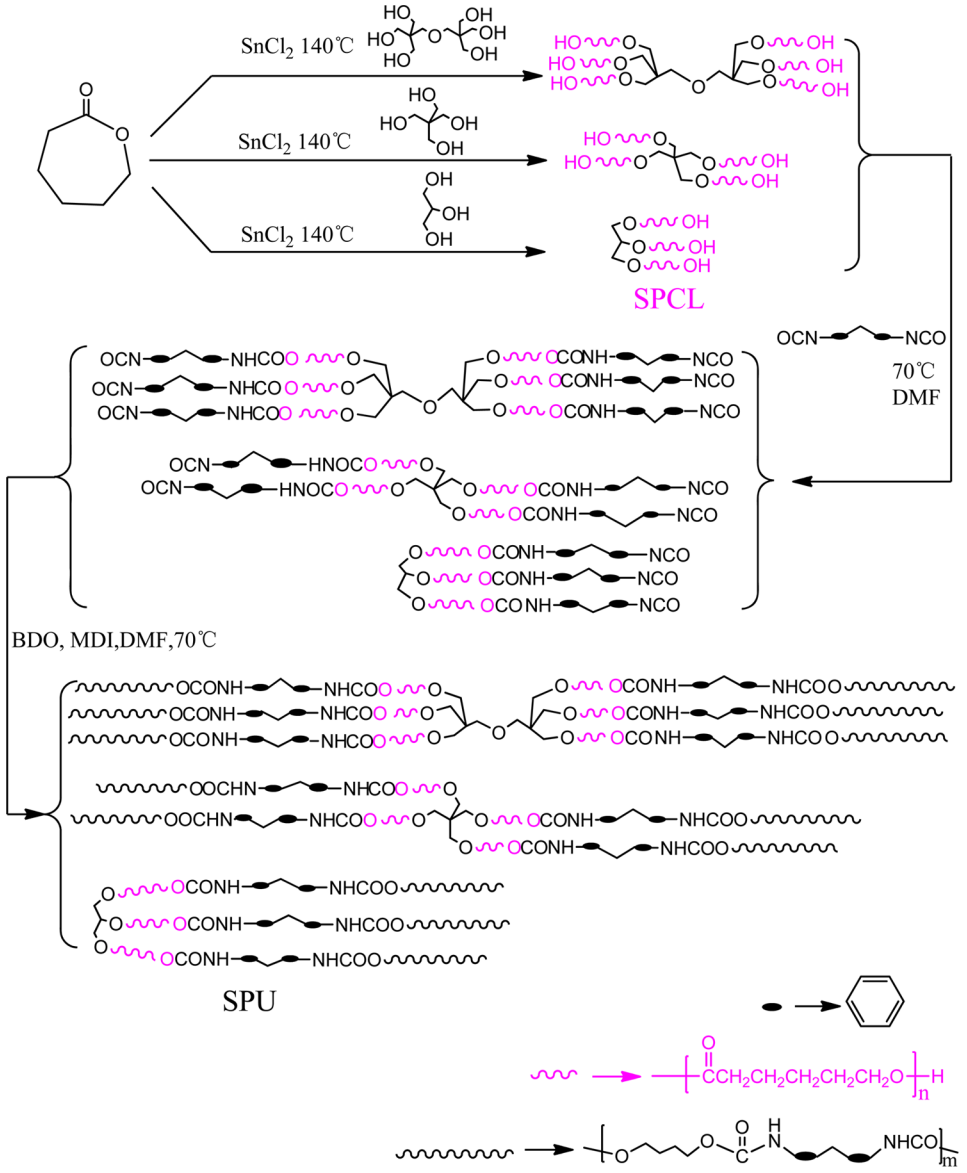

initiators that can form star-shaped polymer are pentaerythritol (PER) and dipentaerythriol (DPE).

Usually the classical shape memory polyurethanes (SMPU) are the dual-shape memory polymer that can be thermally triggered after tensile deformation and fixing of the corresponding shape and it has only one temporary shape.[22] However, triple-shape memory polymer (TSMP), which have most recently been developed, can remember two temporary shapes,[26] for example, the sample can be deformed into a stable state "A" after a two-fold program and recover opposed to the deformation direction from that "low temperature" shape to the "mid-temperature" shape "B", and finally from shape "B" into a high temperature shape "C" upon gradual heating.[5,6] Generally, TSMP are the polymers that have a wide range of temperature change[8,27] or have clear differences between two deformation temperatures.[7,28,26]According to these, TSMP may be exploited in intelligent medical devices and assembling systems.[29]

In this study, to engineer the shape memory polyurethane with more functional groups in a small volume, remarkable shape cycles-averaged shape memory properties and triple-shape memory property, we designed star-shaped shape memory polyurethane. First, we synthesized three kinds of star-shaped poly(ε-caprolactone) (SPCL) with glycol, PER, and DPE, respectively, as initiator, which initiated ε-CL for the ring-opening polymerization (ROP). Then the SPU with different arm numbers were prepared using SPCL as the soft segment and chain-extending with the help of 4,4′-diphenyl methane diisocyanate (MDI) and 1,4-butylene glycol (BDO) as the hard segment. On the one hand, the star architecture would promote the completeness of the freezing of chain segment motion, therefore achieving a higher shape fixed ratio as previously reported.[30] And more internal stress might be stored during the deformation because twining of polymer chains made the relaxation stress elapse more slowly.[30,31] On the other hand, the star structure may prevent the crystallization of soft segment PCL and act as the physical cross-linking points to make the polymer possess triple-shape memory effect.[21,24]

dx.doi.org/10.1021/am5001344 | ACS Appl. Mater. Interfaces 2014, 6, 6545−6554

Table 1. Characterization of the SPCL[a]

		ratio	yield[c] (%)	M_n[a]	T_m (°C)	T_c (°C)	X_c (%)[b]
3S-PCL	CL-G	45-1	77 ± 1	5800 ± 200	51.48	25.96	60 ± 1
4S-PCL	CL-PE	60-1	70 ± 1	8800 ± 300	50.05	26.23	62 ± 1
6S-PCL	CL-DPE	90-1	78 ± 2	11100 ± 200	52.06	32.97	65 ± 1

[a]G for Glycerol, PE for Pentaerythritol, DPE for Depentaerythritol; M_n[a] was determined by ^{1}H-NMR with $CDCl_3$ as the solvent; X_c[b] was calculated according to the equation $X_c = (\Delta H_m/\Delta H_{100\%}) \times 100\%$, where $\Delta H_{100\%}$ is the theoretical heat of fusion of PCL (135 J/g). a, b, and c were expressed as mean ± standard deviation.

EXPERIMENTAL SECTION

Materials. Ethylene glycol (EG, Aldrich) and BDO (Aldrich, 99.5%) were dried with calcium hydroxide (CaH_2) for 24 h and filtered out before use. Glycerol (99%, Tansoole) was dried by azeotropic distillation in toluene before use. N,N-Dimethylformamide (DMF, 99%, Kelong in Chengdu (China)) and ε-CL (99.9%, Aldrich) were distilled over freshly powdered CaH_2 under a reduced pressure. PER and DPE were recrystallized before use. MDI was purchased from Tokyo Chemical Industry Co. LTD and was used without further treatment. Stannous octoate ($Sn(Oct)_2$, 95%) and Stannous chloride ($SnCl_2$) were separately purchased from Aldrich and Kelong chemical reagent factory in Chengdu (China).

Synthesis of Star-Shaped Poly(ε-caprolactone) (SPCL). The ring-opening polymerization method was used to prepare SPCL (Scheme 1). First, a certain amount of ε-CL, initiator and catalyst $SnCl_2$ were put into a single flask quickly. Later, the single flask with a stopcock, which was preheated to remove the moisture, was vacuumized for 4 h with continuous stir to produce a well-mixed molten phase. Finally, the reaction system was put into an air-oven at 140 °C for 6 h. The single flask was cooled after desired reaction time. The resultant polymer was dissolved in dichloromethane (CH_2Cl_2) and precipitated in an excess of cold ethyl alcohol under constant stir. For example, 8 g of CL, 0.198 g of DPE, and 0.08 g of $SnCl_2$ were added into a 50 mL single flask. Then the polymerization was carried out for 6 h at 140 °C. The product was dissolved in 20 mL of CH_2Cl_2 and precipitated in 80 mL of cold ethyl alcohol. The precipitate was dried under a vacuum at room temperature for 24 h. In this way, the obtained polymer was named six-arm poly(ε-caprolactone), i.e., 6S-PCL, whereas the SPCL that was initiated by PER was named four-arm poly(ε-caprolactone), i.e., 4S-PCL, and gycerol's initiated product was named 3S-PCL.

Synthesis of Star-Shaped Polyurethane (SPU). The synthetic route of SPU was also shown in Scheme 1. Quantitative SPCL were added into a 100 mL three-necked round flask and were dried at vacuum under a reduced pressure at 80 °C for 2 h. Then DMF and MDI were successively added into flask with reaction time for 6 h at 60 °C under magnetic stirring to prepare the pre-polymer. After that, chain extender BDO and MDI were added into the reaction system for 24 h at 60 °C. Finally, the stoichiometric ethanol was added dropwise into the flask for terminating. The excessive DMF of the mixture was removed through vacuum rotary evaporation and the acquired viscous mixture was poured into a Teflon dish and then dried at 50 °C for 6 h, and the cast film was then further dried under 80 °C vacuum. The obtained crude film was washed with ethanol to remove uncoupled isocyanate group. According to the above general procedure for star-shaped polyurethane, three-arm polyurethane was prepared. 3S-PCL (1 g) was added in a three-necked flask and dried for 2 h. MDI (0.13 g) and DMF (10 mL) were put into the flask and reacted for 6 h at 60 °C under argon. Then chain extender BDO (0.194 g) and MDI (0.47 g) were added in the reaction system for 24 h. After stopping the reaction, ethanol (5 mL) was added drop wise into the flask. Through vacuum rotary evaporation and solvent evaporation the film was obtained named 3S-PU. While the star-shaped polyurethane prepared by 4S-PCL was named 4S-PU, by 6S-PCL named 6S-PU.

Characterization. *Differential Scanning Calorimetry (DSC).* The thermal properties of these films were analyzed using DSC (TA DSC-Q100). Nitrogen was used as purge gas. Samples were heated from −10 °C to 80 °C with a heating rate of 10 °C/min, cooled down to −20 °C with a cooling rate of −10 °C/min, and then heated to 80 °C again with the same heating rate. Each sample was repeated three times. The melting temperature (T_m) and crystallization temperature (T_c) of the sample were obtained from the second heating curves.

Nuclear Magnetic Resonance (NMR). ^{1}H NMR spectra were recorded with a Bruker AM-300 spectrometer. Tetramethylsilane (TMS) was used as the internal standard and $CDCl_3$ was used as solvent for star-shaped PCL, whereas for star-shaped polyurethane, the solvent is DMSO. The spectra collection was repeated three times for each sample.

Fourier Transform Infrared Spectroscopy (FT-IR). FT-IR was recorded on a Nicolet 5700IR spectrometer. All samples were obtained by KBr plates in which dry polymer power was mixed with KBr at a weight ratio of 0.5−1%.

X-ray Diffractometry (XRD). XRD (Phlips X'Pert PRO, Netherlands) was used to measure the crystallization degree of both star-shaped PCL and star-shaped PU. The measurement was repeated three times for each sample. The scanning rage is 10−60°. Firstly, the sample was heated from 10 to 100°, and the message was then recorded when the desired temperature was reached during the cooling process.

Static Tensile Test. Static tensile test was performed at the cross-head speed of 2 mm min^{-} at room temperature using a universal testing machine Instron 5567 (Instron Co. , Massachusetts). The test was repeated three times for each sample.

Dynamic Mechanical Thermal Analysis (DMA). Dynamic mechanical properties were determined by a DMA (DMA-Q800, TA, USA), in the tensile resonant mode, at a heating rate of 3 °C/min from −20 °C to 80 °C and at a frequency of 1 Hz. The storage modulus E' and loss factor tan δ were gained. The analysis was repeated three times for each sample.

In Vitro Cytotoxicity Assay. The cytotoxicity assay was evaluated on the basis of the Alamar blue assay as previously reported.[42] The osteoblast cells employed belong to normal cell line, which were from neonatal rat's mandibular. They have been passaged to the third generation just before our experiments. In brief, all samples were cut into small round flake at an average diameter of nearly 12 mm for culture with osteoblasts in vitro. After that, osteoblasts were grown in RPMI medium 1640 (Gibcos) with 10% fetal bovine serum (FBS). These cells with a density of 1×10^4 cells/well were cultured in a 24-well plate (Sigma) in the above medium and maintained at 37 °C in a humidfied incubator with 5% CO_2. At the predesigned time points of 1, 3, and 5 days, the medium was removed and 300 μL of Alamar blue solution (10% Alamar blue, 80% media 199 (Gibcos) and 10% FBS; v/v) was added into each well and incubated for further 3 h. Blank controls were wells without materials. A sample of 200 μL of reduced Alamar blue solution was pipetted into a costar opaque black bottom 96-well plate (Sigma) and read at 570 (excitation)/600 (emission) in an ELISA microplate reader (Molecular Devices, Sunnyvale, CA). Cell morphology and growth on SPU films were detected by optical microscopy (ZEISS Axio Imager A1 m).

RESULTS AND DISCUSSION

Characterization of SPCL. SPCL were prepared by ring-opening polymerization (ROP) with stoichiometric as shown in Table 1. To verify the successful preparation of SPCL, the structure of SPCL were investigated through ^{1}H-NMR. The ^{1}H-NMR spectra of 3S-PCL, 4S-PCL, and 6S-PCL were shown in Figure 1. In the ^{1}H-NMR spectrum of 3S-PCL-45, the

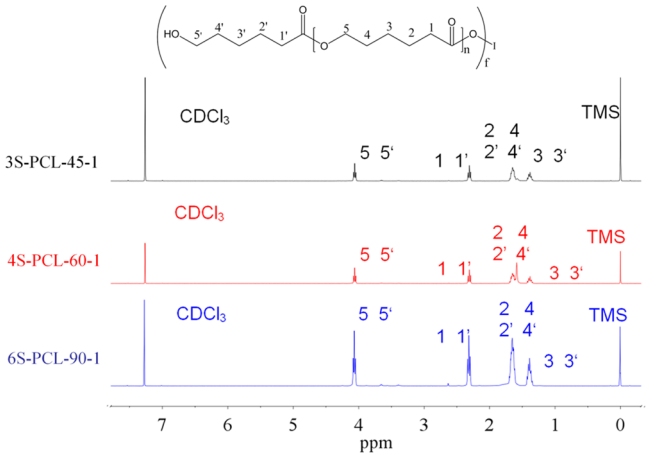

Figure 1. ^{1}H- NMR of SPCL.

disappearance of OH signal (4.7 ppm) from glycerol indicates the reaction of OH groups with ε-CL,[3] whereas H-(3,3′) at 2.25−2.35 ppm, H-(2,2′,4,4′) at 1.59−1.71 ppm, H-(3,3′) at 1.35−1.42 ppm, H-(5) at 4.05−4.1 ppm, H-(5′) at 3.65−3.69 ppm, all chemistry shift signals matched with the corresponding protons, indicate the successful preparation of 3S-PCL.[8] For the 4S-PCL and 6S-PCL, each signal is also assigned to the corresponding proton of the proposed structure, suggesting the successful synthesis of star-shaped PCL. And from the intensity of signal H-(5′) and H-(5), the repeating unit n was calculated and then M_n was deduced. Previously, it was found that the linear poly(ε-caprolactone)-polyurethane (LPCLU) whose PCL has a M_n less than 2000 would be noncrystalline.[33] The crystallization of LPCLU was attributed to the PCL segments since the MDI-EG hard segments usually not crystallize.[34] And as M_n of PCL is 3000, the T_m of LPCLU is 48.5 °C, which is 10 °C lower than the T_m of PCL-3000.[33] Therefore, to ensure the transition temperature (T_{trans}) of SPU close to body temperature, we targeted preparing a series of SPCL with M_n for every chain of 1500 as shown in Table 1, with mole ratios of 45-1 for CL-G, 60-1 for CL-PE, and 90-1 for CL-DPE. The thermal properties of SPCL were studied by DSC and listed in Table 1. As shown in Table 1, as the arm numbers of star-shaped PCL increases, T_m, T_c, and M_n have a tendency to increase.

Characterization of SPU. SPU was synthesized from SPCL and MDI, with BDO as the chain extender (Scheme 1). To indicate the structure of SPU, we used FT-IR and ^{1}H-NMR. The urethane formation in 3S-PU, 4S-PU, and 6S-PU is confirmed by the appearance of urethane linkage (ν-NHCO) at 1520 cm^{-1} and the disappearance of NCO group at 2200 cm^{-1}, and the double-peak of benzene ring at 1500 cm^{-1} also demonstrates the synthesis of star-shaped PU (Figure 2A). Figure 2B shows the typical ^{1}H-NMR of 6S-PU. The signals at c (7.47 ppm) and d (7.23 ppm) are contributed to the H of benzene ring, a (9.18 ppm) for the N−H of urethane, which all indicated the successful preparation of 6S-PU. The signals at 1.2−1.4 ppm for H-(3,3′), 1.5−1.65 ppm for H-(2,2′,4,4′,7,8), 2.25−2.32 ppm for H-(1,1′), 3.75 ppm for H-(b), and 3.9−4.14 ppm for H-(5,5′,6,9) appeared at the positions as previously reported.[25,35] Through the ratio of NH-(a)/H-(3,3′), the actual reaction degree of (MDI+BDO) can be calculated,[25] and the actual soft segment contention can then be obtained as listed in Table 2.

Thermal Properties of SPU. The thermal properties of SPU with various arm numbers were characterized by DSC.

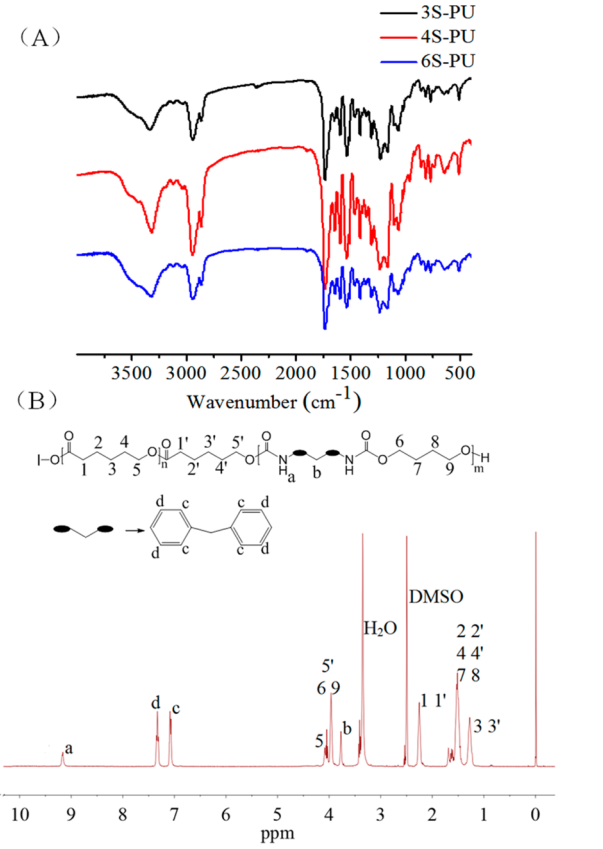

Figure 2. (A) FT-IR of SPU: 3S-PU (black line); 4S-PU (red line); 6S-PU (blue line); (B) ^{1}H-NMR of 6S-PU.

Figure 3 shows the curves of the SPU obtained from the second heating and cooling scanning process, and the T_m and T_c are listed in Table 2. For SPU with the same arm numbers, T_m of 6S-PU decreases from 46 to 41 °C with the decrease in soft segment content from 65 to 55%; meanwhile, the melting range presents an increase with the decrease of soft segment composition as illustrated in Figure 3C. The thermal properties of 3S-PU and 4S-PU are shown in Table 2 and Figure 3, respectively. According to the results of Table 2 and Figure 3, it is easy to find that T_m, T_c and melting range of both 3S-PU and 4S-PU exhibit the same trend as the 6S-PU. These variations of T_m, T_c and melting range are caused by the decreased crystallinity of soft segment PCL and inhibited crystal formation of hard segment as previously reported.[35] For SPU, the star-shaped structure can be used as a physical network point which can improve the mechanical property and shape memory property theoretically.[24] However, for the SPU with the same soft segment ratio as shown in Figure S1 the Supporting Information (SI), both the T_m and T_m region increased with the increase of arm numbers. For instance, 6S-PU-55% possesses a T_m region from 20 to 50 °C. The main reason may be that the restriction from the twining of macromolecule chains to crystallization of soft segment SPCL increases with increase of arm numbers and meanwhile crystallize degree presents a higher trend of imperfection, which gave rise to a broadened melting range.[34,25] On the other hand, the crystallize degree has a much less decrease for the 6S-PU compared with the PU of three arm numbers, which endows the 6S-PU higher T_m. It might be that the number of the star-shaped structure which can be seemed as the physical

dx.doi.org/10.1021/am5001344 | ACS Appl. Mater. Interfaces 2014, 6, 6545−6554

Table 2. Synthesis of SPU by Polymerization of SPCL, MDI, and BDO with Stannous Octoate As Catalyst in DMF[a]

	entry	MDI:BDO:PCL	SS(%)[a]	SS(%)[b]	T_m (°C)	X_c^f (%)
3S-PU	1	14:12:1	55	60 ± 1	36	6.67 ± 0.75
	2	12:10:1	60	68 ± 1	38	
	3	10:8:1	65	70 ± 1	41	
4S-PU	4	18:16:1	55	61 ± 1	41	11.40 ± 1.03
	5	16:14:1	60	65 ± 2	44	
	6	14:12:1	65	71 ± 1	45	
6S-PU	7	28:25:1	55	59 ± 1	44	12.59 ± 0.65
	8	23:20:1	60	64 ± 1	46	
	9	18:15:1	65	69 ± 1	47	

[a]SS[a] for soft segment of SPU, the percentage based on the feed ratio. SS[b] for soft segment of SPU, the percentage based on the practical value determined by ^{1}H-NMR. X_c^f for crystallinity of SPU calculated according to MDI Jade 5. b and f were expressed as mean ± standard deviation.

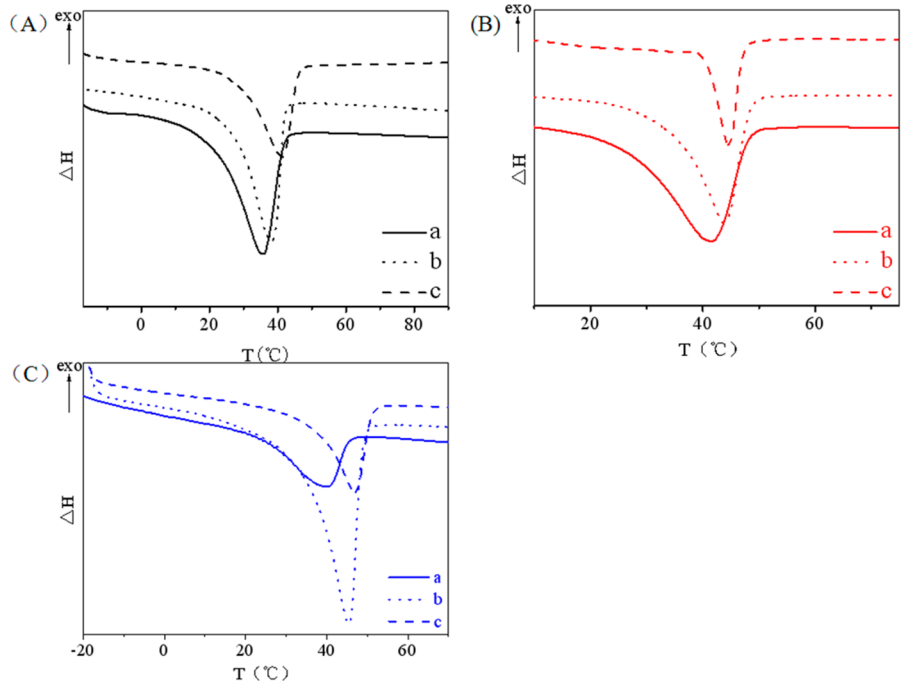

Figure 3. DSC curves of SPU: (A) 3S-PU marked with black; (B) 4S-PU marked with red; (C) 6S-PU marked with blue. Curves a, b, and c represent that the star-shaped polymer contain 55, 60, and 65% of soft segment.

crosslink point for equal soft segment content would present a decrease tendency.[25] Previously, Xie[27] investigated a thermoplastic Nfion polymer with a broad glass transition (T_g) region, and the application of multiple programming steps within the glass transition of the material gave experimental evidence for distinct multi-shape memory behavior. Herein, SPU with broader melting range might have triple shape memory effect with T_{trans} close to body temperature.

Shape Memory Property. Table S1 in the Supporting Information shows the shape memory fixity ratio (R_f) and recovery ratio (R_r) of SPU that obtained from DMA. Equations 1 and 2 show the corresponding calculations for R_f and R_r.[25]

$$R_f = \left(\frac{\varepsilon_u(N)}{\varepsilon_m}\right) \times 100\% \quad (1)$$

$$R_r(N) = \left(\frac{\varepsilon_m - \varepsilon_p(N)}{\varepsilon_m - \varepsilon_p(N-1)}\right) \times 100\% \quad (2)$$

where N denotes the N_{th} cycle, ε_m the maximum strain, $\varepsilon_u(N)$ the temporary strain at N_{th} cycle, and $\varepsilon_p(N)$ the recovery strain at N_{th} cycle.

Both the R_f and R_r increased with increase of soft segment contention at the same arm numbers, which is in good agreement with the results of DSC analysis that a broad melting temperature range was observed from star-shaped PU with soft segment content 55%. The wide temperature range can endow the materials with multiple shape memory effect as reported previously.[27,42] So star-shaped PU with 55% star-shaped PCL was selected as the material for following discussion of shape memory property. Figure 4 (1) shows the storage modulus (E′) and tan δ of 3S-PU-55%, 4S-PU-55%, and 6S-PU-55%. The E' and tan δ vs. temperature of various specimens were measured on a range of temperature between 0 °C and 100 °C. In Figure 4 (1), E′ exhibits two slope plateaus below and above the melting temperature respectively, and the tan δ shows a drastic increase around T_m, indicating better shape memory effect of SPU.[27]

In the temperature region around 5 °C, E′ is at a higher value, and these data unveiled that the polymer are in their

dx.doi.org/10.1021/am5001344 | ACS Appl. Mater. Interfaces 2014, 6, 6545−6554

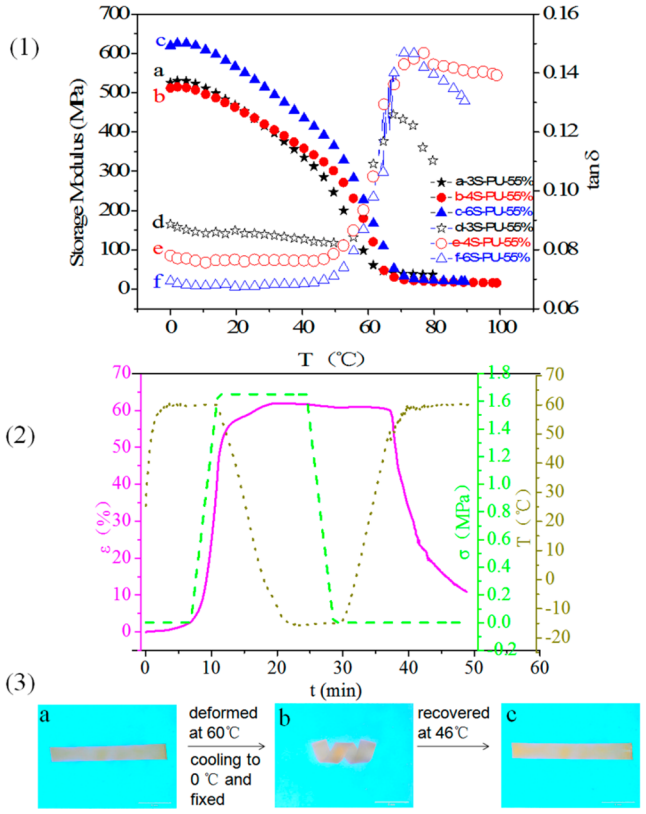

Figure 4. (1) The dynamical mechanical analysis of SPU: a, b, and c for storage modulus; d, e, and f for tan δ. (2) Cyclic thermal mechanical analysis of 6S-PU. The solid line for ε, dash line for σ, dot line for T. (3) The shape memory effect of 6S-PU: (a) initial state; (b) deformed state (deformed at 60 °C and fixed at 0 °C); (c) recovered state after being soaked at 46 °C water for10 s.

semi-crystalline state. E' for these SPU is 627 MPa for 6S-PU-55%, 528 MPa for 4S-PU-55%, and 510 MPa for 3S-PU-55%. Obviously, the E' displays an increasing trend with the increase of arm numbers at low temperature. The possible reason is that the star-shaped structure in the SPU as a physical cross-linking point can make the polymer achieve some elasticity and enhance their stiffness.[30] Moreover, the increase of twining among the molecular chains with the increase of arm numbers, which will impose some more positional restriction on SPU, may be another reason for high storage modulus of SPU with high arm numbers.[8,35] Below T_m, the E' decrease with the increase in temperature could demonstrate the effect of the star-shaped structure. Around T_m of SPCL, the E' of SPU exhibit a drastic decrease, which might be due to the melting of soft segment PCL.[38,37] And the onset T_m in Figure 4 (1) shows that the E' has a relatively slow decrease slope in the temperature range between 5 °C and T_m, which is due to the melt of PCL crystallize of a lower regularity and the removal of twining among molecular chains.[39]

Figure 4 (2) quantitatively shows the dual-shape memory property of 6S-PU determined by DMA. The stripe was firstly heated at 60 °C for 5 min so that it could be softened, and then it was strained at a stress rate of 0.5 MPa/min to 2 MPa, obtained a temporary shape with ε_m for 55%. The temporary shape was fixed by cooling to 0 °C, releasing the stress and the strain ε_u obtained. After keeping the temporary shape for 5 min, the stripe was heated again to 60 °C for 10 minutes and the temporary shape was recovered to gain the strain ε_p.

An increase in the R_f and R_r of the three kinds of polyurethane with different arm numbers was further observed following the increase of the arm numbers. Because the polyurethane has microphase separation structure, the crystallize of soft segment PCL is used as reversible phase to fix the temporary shape, whereas the elasticity of hard segment of PU can be utilized to recover its original shape as previously reported.[28,29] Identically, the shape fixing of the star-shaped PU is also due to the crystallization of the soft segment star-shaped PCL while the shape recovery is mainly because of the elasticity of PU.[25,31] However, the star-shaped structure existing in PU make the molecular chains contact each other more easily and twine around each other more closely, which would offer some help to the shape recovery and this help will increase with the increase of arm numbers.[43] At the same time, the number of the star-shaped structure, which can be regarded as a physical crosslink point,[34] would increase as the SPU having the same soft segment ratio with the decrease of the arm amount and in turn increase the degree of cross linking. Consequently, the crystalline degree of the soft segment was decreased, leading to the shape fixed ratio decreasing. Figure 4 (3) shows the macroscopic dual-shape memory process of 6S-PU. Firstly the sample was heated at 60 °C for 1 min, then deformed it to spiral, cooled to 0 °C, and released the stress at last. After keeping the temporary shape for 5 min, heating the sample to 46 °C, the spiral temporary shape recovered its original shape in 10 s.

According to the results of DSC and DMA, we can clearly find that 6S-PU has a wide transition temperature that can endow it with triple shape memory effect. Figure 5 (1) shows cyclic thermal mechanical analysis of 6S-PU-55% measured by DMA. First, we strained the specimen (shape A) at a stress rate of 0.5 MPa/min to 2 MPa at 70 °C, and obtained a temporary shape I (shape B) that was marked as $\varepsilon_{s1I\text{-}F}$; we then cooled it to 40 °C and released the stress, marked as ε_{s1I}. Secondly, strained the specimen of shape B at a same stress rate to obtain another temporary shape II (shape C), marked as $\varepsilon_{s2II\text{-}F}$, and then cooled to 0 °C and released the stress, marked as ε_{S2II}. Finally, the temporary shape II (shape C) was heated in 40 °C to recover to the shape D, the strain marked as $\varepsilon_{SI,R}$, and the specimen was then further heated to 70 °C to recover to the initial shape E, the strain marked as $\varepsilon_{S0,R}$. The shape memory fixity ratio and recovery ratio were calculated according to the following equations

$$R_f(0 \rightarrow I) = \frac{\varepsilon_{SI}}{\varepsilon_{SI\text{-}F}} \times 100\% \quad (3)$$

$$R_f(I \rightarrow II) = \left(1 - \frac{\varepsilon_{SII\text{-}F} - \varepsilon_{SII}}{\varepsilon_{SII\text{-}F} - \varepsilon_{SI}}\right) \times 100\% \quad (4)$$

$$R_r(II \rightarrow I) = \frac{\varepsilon_{SII\text{-}F} - \varepsilon_{SI,R}}{\varepsilon_{SII\text{-}F} - \varepsilon_{SI}} \times 100\% \quad (5)$$

$$R_r(I \rightarrow 0) = \left(1 - \frac{\varepsilon_{S0,R}}{\varepsilon_{SI}}\right) \times 100\% \quad (6)$$

The R_f (0→ I) and R_f (I → II) could reach 90 and 99%, respectively, whereas the R_r (II → I) and R_r (I → 0) can reach 99 and 93% respectively. Figure 5(2) shows the macroscopic triple shape memory process of 6S-PU-55% which further indicated better triple shape memory effect of 6S-PU. Firstly, the stripe was deformed to a V shape (temporary shape I) at

dx.doi.org/10.1021/am5001344 | ACS Appl. Mater. Interfaces 2014, 6, 6545−6554

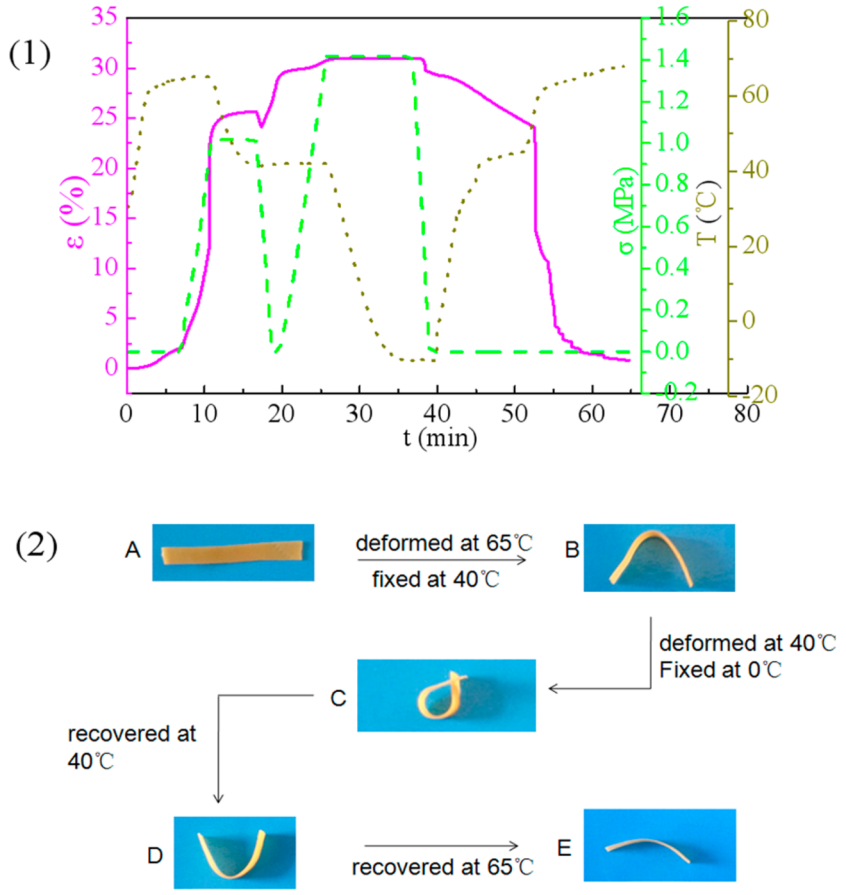

Figure 5. Triple-shape memory effect of 6S-PU-55% based on the broadened T_m range. (1) The cyclic thermal mechanical analysis of 6S-PU instructed by Dynamic thermal-mechanical analyzer. The solid line for ε, dash line for σ, dot line for T. (2) These pictures show the shape memory process of 6S-PU: A (the permanent shape), B (the temporary shape I deformed at 70 °C and fixed at 40 °C), C (the temporary shape II deformed at 40 °C and fixed at 0 °C), D (recover the temporary shape I at 40 °C water for 5 seconds), E (recover to the initial shape at 65 °C water for 10 seconds), R_f (A→B): 90%; R_f (B→C): 99%; R_r (C→D): 99%; R_r (B→E): 93%.

70 °C and fixed at 40 °C for 1 min; the specimen was then deformed to a ring (temporary shape II) and fixed at 0 °C for 5 min. After that, the temporary shape II was recovered under the polymer immersing in 40 °C water for 10 s; the temporary shape I was restored after immersing in 70 °C water for 10 s.

Mechanism of Triple-Shape Memory Effect. From above discussion, we could assert that the changes of the microstructure and molecular chain play important roles in influencing the shape memory effect of SPU. XRD was carried out to study the degree of crystalline (Figure 6A), whereas Figure 6B interprets the mechanism of shape memory process from the molecular level. As shown in Figure 6A, pure SPCL exhibits strong reflections at 2θ values of 21.37, 22.05, and 23.77° corresponding to (110), (111), and (200) reflections.[44] These reflection peaks of the SPCL agree with the reported unit cell parameters of PCL.[45] These reflections appeared in SPU and the reflecting positions were consistent with SPCL though reflect intensity decreased greatly, which demonstrated crystallization existing in SPU. However, the degree of crystallinity increased slightly with the increase in arm numbers. As shown in Figure 6B, the twining among molecular chains, the star-shaped structure which can be used as physical points, would endow the polymer a wider T_m range, providing triple shape memory effect. When heated to 65 °C, the soft segment SPCL melted completely, and the twining among molecular chains was removed, and thus all the molecular chains were in a situation of freely extending and then the material can be deformed easily.

After cooling to 40 °C, the partial soft segments began to crystallize firstly and could fix some strain, i.e. temporary shape B. In the process of shape A to shape B, the star-shaped structure and molecular twining are used as fixed phase, while the partial crystalline soft segment as reversible phase. And then the other PCL chains would crystallize fully and the movement of hard segment is restricted following the decrease of temperature to obtain final temporary shape C. In the process of shape B to shape C, the hard segment is used as fixed phase, and the soft segment PCL crystallizing fully as reversible phase. During the shape recovery, as heating to 40 °C, the molecular twining would be removed and some imperfect PCL crystallization would melt firstly to recover some strain to get temporary shape B. Further heating the polymer to 65 °C, the SPCL crystallization would melt completely and the initial shape could be obtained.

Mechanical Property. Figure 7 shows the mechanical properties such as the tensile stress, strain, and Young's modulus of SPUs. From the results of stress-strain curves, the maximum tensile stress increased with the increase of arm numbers with the same soft segment for 55%. The reason could be that the higher crystallinity of 6S-PU supplies the polymer stronger stiffness, and the molecular twining among 6S-PU is also an important factor for the maximum tensile stress.

dx.doi.org/10.1021/am5001344 | ACS Appl. Mater. Interfaces 2014, 6, 6545−6554

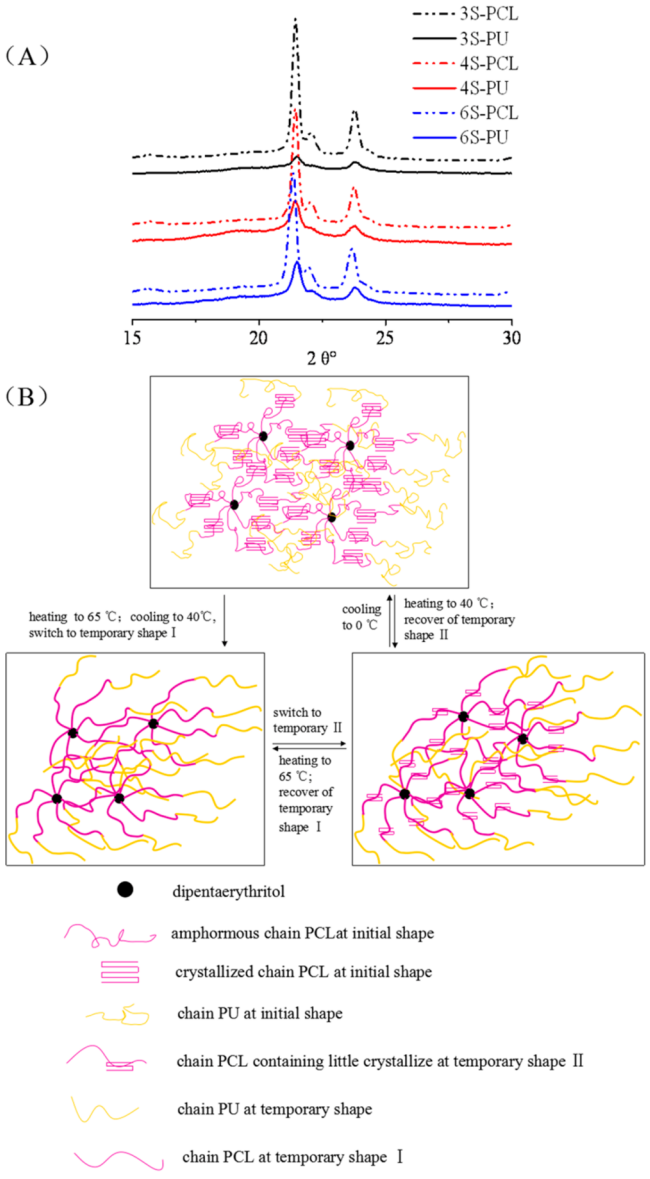

Figure 6. (A) XRD curves of SPCL and SPU; (B) the mechanism of triple shape memory effect of 6S-PU.

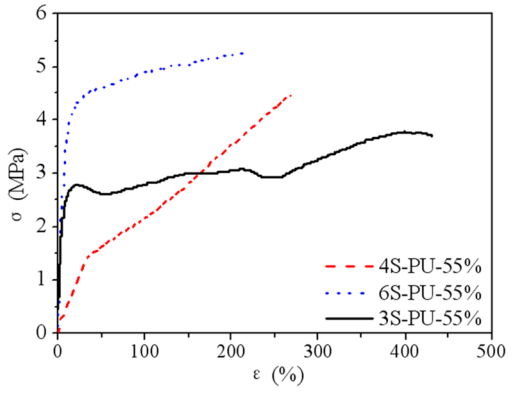

Figure 7. Mechanical properties of SPU.

Additionally, the elongation increased with the decrease of the arm numbers for these polymers.[23]

In Vitro Cytotoxicity Analysis. The ability to provide cells attachment and proliferation is an important characteristic for biomaterials. Osteoblasts are cultured to evaluate the biocompatibility of the synthesized star-shaped PU based on Alamar blue assay according to the previously reported.[26] From Figure 8A,where all the data were presented as mean ± standard deviation (SD), it can be clearly found that cell viability for all specimens is more than 80% at first day. After culture of 3 days and 5 days, the cell viability for all specimens is more than 95% with no obvious significant difference. To further demonstrate the result of Alamar blue assay, the morphology of osteoblasts is observed by optical microscopy as shown in Figure 8B. It can be found that the osteoblasts grew healthily and attached well on the all star-shaped PU films. All of these results suggest that these polymers possess good cytocompatibility. Consequently, these materials can be potentially used as biomaterials. In particular, they can be used as smart medical devices. The shape memory function can be utilized to make a bulky SPU implant be fabricated into a small shape, and thus it can be easily placed in body through small wounds.[10,16]

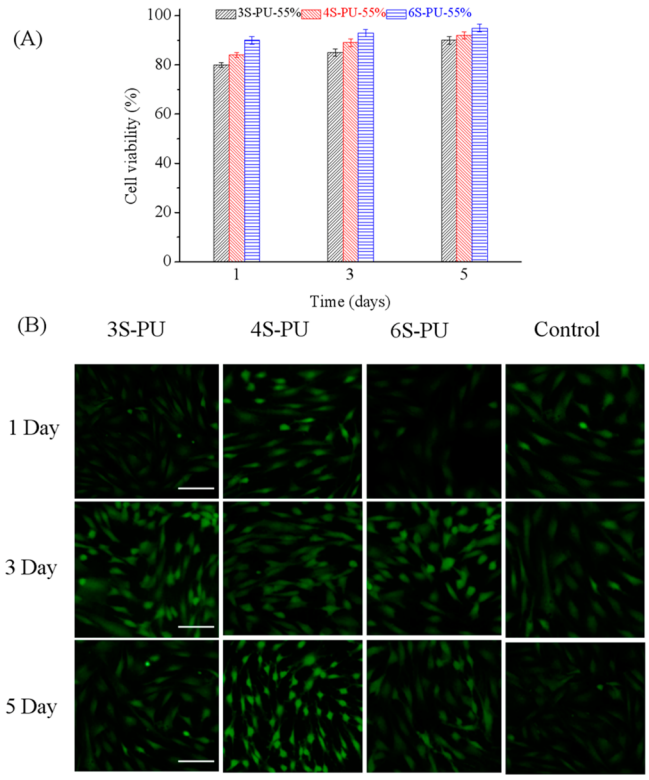

Figure 8. (A) Alamar blue analysis and optical microscope images; (B) osteoblasts cultured on SPU films with different arm numbers at day 1, 3, and 5, respectively. All the scale bars represent 50 μm.

CONCLUSIONS

In summary, a series of star-shaped polyurethane were prepared successfully based on star-shaped PCL with three, four, and six arm numbers. 6S-PU has a better shape memory effect than 4S-PU and 3S-PU with a same ratio of hard segment. In the polymer, the star-shaped structure and the molecular twining were used as the fixed phase, while the partial crystalline soft segment as the reversible phase. The increase of the crystallinity of SPU with the increase of the arm numbers endowed 6S-PU

high shape fixity and a wide melting temperature range, which led 6S-PU to achieve an excellent triple-shape memory effect. Cytotoxicity analysis demonstrated that the polymer possesses good cytocompatibility. Therefore, the 6S-PU is potentially developed for biomedical applications.

■ ASSOCIATED CONTENT

Supporting Information

The thermal properties of 3S-PU, 4S-PU, and 6S-PU and the three kinds of SPU with the equal soft segment content are shown in Figure S1. Both the T_m and T_m range present an increase tendency with the increase of arm numbers. Table S1 shows shape memory property of SPU with different arm numbers and different soft segment compositions. This material is available free of charge via the Internet at http://pubs.acs.org/.

■ AUTHOR INFORMATION

Corresponding Author

*E-mail:shaobingzhou@hotmail.com or shaobingzhou@swjtu.cn.

Notes

The authors declare no competing financial interest.

■ ACKNOWLEDGMENTS

X.Y. and L.W. contributed equally to this work.This work was partially supported by National Basic Research Program of China (973 Program, 2012CB933600), National Natural Science Foundation of China (51173150, 51373138), Research Fund for the Doctoral Program of Higher Education of China (20120184110029), and Construction Program for Innovative Research Team of University in Sichuan Province (14TD0050).

■ REFERENCES

(1) Behl, M.; Razzaq, M. Y.; Lendlein, A. Multifunctional Shape-Memory Polymers. *Adv. Mater.* **2010**, *22*, 3388−3410.

(2) Luo, X.; Mather, P. T. Preparation and Characterization of Shape Memory Elastomeric Composites. *Macromolecules* **2009**, *42*, 7251−7253.

(3) Zheng, X.; Zhou, S.; Li, X.; Weng, J. Shape Memory Properties of Poly(D,L-lactide)/Hydroxyapatite Composites. *Biomaterials* **2006**, *27*, 4288−4295.

(4) Yu, X.; Zhou, S.; Zheng, X.; Guo, T.; Xiao, Y.; Song, B. a Biodegradable Shape-Memory Nanocomposite with Excellent Magnetism Sensitivity. *Nanotechnology* **2009**, *20*, 235702.

(5) Shi, Y.; Yoonessi, M.; Weiss, R. A. High Temperature Shape Memory Polymers. *Macromolecules* **2013**, *46*, 4160−4167.

(6) Ahn, S. K.; Kasi, R. M. Exploiting Microphase-Separated Morphologies of Side-Chain Liquid Crystalline Polymer Networks for Triple Shape Memory Properties. *Adv. Funct. Mater.* **2011**, *21*, 4543−4549.

(7) Cuevas, J. M.; Rubio, R.; Germán, L.; Laza, J. M.; Vilas, J. L.; Rodriguez, M.; León, L. M. Triple-Shape Memory Effect of Covalently Crosslinked Polyalkenamer Based Semicrystalline Polymer Blends. *Soft Matter* **2012**, *8*, 4928−4935.

(8) Bothe, M.; Mya, K. Y.; Lin, E. M. J.; Yeo, C. C.; Lu, X.; He, C.; Pretsch, T. Triple-Shape Properties of Star-Shaped POSS-Polycaprolactone Polyurethane Networks. *Soft Matter* **2012**, *8*, 965−972.

(9) Sauter, T.; Lützow, K.; Schossig, M.; Kosmella, H.; Weigel, T.; Kratz, K.; Lendlein, A. Shape-Memory Properties of Polyetherurethane Foams Prepared by Thermally Induced Phase Separation. *Adv. Eng. Mater.* **2012**, *14*, 818−824.

(10) El Feninat, F.; Laroche, G.; Fiset, M.; Mantovani, D. Shape Memory Materials for Biomedical Applications. *Adv. Eng. Mater.* **2002**, *4*, 91.

(11) Pretsch, T.; Ecker, M.; Schildhauer, M.; Maskos, M. Switchable Information Carriers Based on Shape Memory Polymer. *J. Mater. Chem.* **2012**, *22*, 7757−7766.

(12) Matsumoto, H.; Ishiguro, T.; Konosu, Y.; Minagawa, M.; Tanioka, A.; Richau, K.; Kratz, K.; Lendlein, A. Shape-Memory Properties of Electrospun Non-Woven Fabrics Prepared from Degradable Polyesterurethanes Containing Poly(ω-pentadecalactone) Hard Segments. *Eur. Polym. J.* **2012**, *48*, 1866−1874.

(13) Metcalfe, A.; Desfaits, A.; Salazkin, I.; Yahia, L. H.; Sokolowski, W. M.; Raymond, J. Cold Hibernated Elastic Memory Foams for Endovascular Interventions. *Biomaterials* **2003**, *24*, 491−497.

(14) Metzger, M. F.; Wilson, T. S.; Schumann, D.; Matthews, D. L.; Maitland, D. J. Mechanical Properties of Mechanical Actuator for Treating Ischemic Stroke. *Biomed. Microdevices* **2002**, *4*, 89−96.

(15) Daniels, A. U.; Chang, M. K.; Andriano, K. P.; Heller, J. Mechanical Properties of Biodegradable Polymers and Composites Proposed for Internal Fixation of Bone. *J. Appl. Biomater.* **1990**, *1*, 57−78.

(16) Lendlein, A.; Langer, R. Biodegradable, elastic shape-memory polymers for potential biomedical applications. *Science* **2002**, *296*, 1673−1676.

(17) Wang, L.; Shansky, J.; Borselli, C.; Mooney, D.; Vandenburgh, H. Design and Fabrication of a Biodegradable, Covalently Crosslinked Shape-Memory Alginate Scaffold for Cell and Growth Factor Delivery. *Tissue Eng., Part A* **2012**, *18*, 2000−2007.

(18) Lendlein, A.; Behl, M.; Hiebl, B.; Wischke, C. Shape-Memory Polymers As a Technology Platform for Biomedical Applications. *Expert Rev. Med. Devices* **2010**, *7*, 357−379.

(19) Hu, J.; Yang, Z.; Yeung, L.; Ji, F.; Liu, Y. Crosslinked Polyurethanes with Shape Memory Properties. *Polym. Int.* **2005**, *54*, 854−859.

(20) Lendlein, A.; Kelch, S. Shape-Memory Effect. *Angew. Chem., Int. Ed.* **2002**, *41*, 2034−2057.

(21) Behl, M.; Bellin, I.; Kelch, S.; Wagermaier, W.; Lendlein, A. One-Step Process for Creating Triple-Shape Capability of AB Polymer Networks. *Adv. Funct. Mater.* **2009**, *19*, 102−108.

(22) Inoue, K. Functional Dendrimers, Hyperbranched, and Star Polymers. *Prog. Polym. Sci.* **2000**, *25*, 453−571.

(23) Matyjaszewski, K.; Miller, P. J.; Pyun, J.; Kickelbick, G.; Diamanti, S. Synthesis and Characterization of Star Polymers with Varying Arm Number, Length, And Composition from Organic and Hybrid Inorganic/Organic Multifunctional Initiators. *Macromolecules* **1999**, *32*, 6526−6535.

(24) Mya, K. Y.; Gose, H. B.; Pretsch, T.; Bothe, M.; He, C. Star-Shaped POSS-Polycaprolactone Polyurethanes and Their Shape Memory Performance. *J. Mater. Chem.* **2011**, *21*, 4827−4836.

(25) Xue, L.; Dai, S.; Li, Z. Synthesis and Characterization of Three-Arm Poly(ε-caprolactone)-Based Poly(ester-urethanes) with Shape-Memory Effect at Body Temperature. *Macromolecules* **2009**, *42*, 964−972.

(26) Wang, L.; Yang, X.; Chen, H.; Gong, T.; Li, W.; Yang, G.; Zhou, S. Design of Triple-Shape Memory Polyurethane with Photo-cross-linking of Cinnamon Groups. *ACS Appl. Mater. Interfaces* **2013**, *5*, 10520−10528.

(27) Xie, T. Tunable polymer multi-shape memory effect. *Nature* **2010**, *464*, 267−270.

(28) Chung, Y. C.; Khiem Nguyen, D.; Won Choi, J.; Chul Chun, B. The Effect of Soft Segment Content and Linker Length on Shape Recovery and Mechanical Properties of Laterally Linked Polyurethane Copolymer. *J. Appl. Polym. Sci.* **2011**, *120*, 2063−2073.

(29) Chen, S.; Hu, J.; Zhuo, H.; Chen, S. Effect of MDI−BDO hard segment on pyridine-containing shape memory polyurethanes. *J.Mater. Sci.* **2011**, *46*, 5294−5304.

(30) Liu, T.; Li, J.; Pan, Y.; Zheng, Z.; Ding, X.; Peng, Y. A New Approach to Shape Memory Polymer: Design and Preparation of Poly(methyl methacrylate) Composites in the Presence of Star Poly(ethylene glycol). *Soft Matter* **2011**, *7*, 1641−1643.

(31) Xue, L.; Dai, S.; Li, Z. Synthesis and Characterization of Elastic Star Shape-Memory Polymers As Self-Expandable Drug-Eluting Stents. *J. Mater. Chem.* **2012**, *22*, 7403−7411.
(32) Shao, S.; Zhou, S.; Li, L.; Li, J.; Luo, C.; Wang, J.; Li, X.; Weng, J. Osteoblast Function on Electrically Conductive Electrospun PLA/MWCNTs Nanofibers. *Biomaterials* **2011**, *32*, 2821−2833.
(33) Ping, P.; Wang, W.; Chen, X.; Jing, X. Poly(ε-caprolactone) Polyurethane and Its Shape-Memory Property. *Biomacromolecules* **2005**, *6*, 587−592.
(34) Born, L.; Hespe, H.; Crone, J.; Wolf, K. H. The Physical Crosslinking of Polyurethane Elastomers Studied by X-ray Investigation of Model Urethanes. *Colloid Polym. Sci.* **1982**, *260*, 819−828.
(35) Xue, L.; Dai, S.; Li, Z. Biodegradable Shape-Memory Block Co-Polymers for Fast Self-Expandable Stents. *Biomaterials* **2010**, *31*, 8132−8140.
(36) Lendlein, A.; Zotzmann, J.; Feng, Y.; Alteheld, A.; Kelch, S. Controlling the Switching Temperature of Biodegradable, Amorphous, Shape-Memory Poly(rac-lactide) Urethane Networks by Incorporation of Different Comonomers. *Biomacromolecules* **2009**, *10*, 975−982.
(37) Chen, S.; Hu, J.; Zhuo, H.; Yuen, C.; Chan, L. Study on the Thermal-Induced Shape Memory Effect of Pyridine Containing Supramolecular Polyurethane. *Polymer* **2010**, *51*, 240−248.
(38) Zhu, Y.; Hu, J.; Yeung, K. Effect of Soft Segment Crystallization and Hard Segment Physical Crosslink on Shape Memory Function in Antibacterial Segmented Polyurethane Ionomers. *Acta Biomater.* **2009**, *5*, 3346−3357.
(39) Bellin, I.; Kelch, S.; Langer, R.; Lendlein, A. Polymeric Triple-Shape Materials. *Proc. Natl. Acad. Sci. U.S.A.* **2006**, *103*, 18043−18047.
(40) Shao, Y.; Lavigueur, C.; Zhu, X. X. Multishape Memory Effect of Norbornene-Based Copolymers with Cholic Acid Pendant Groups. *Macromolecules* **2012**, *45*, 1924−1930.
(41) Zhao, J.; Chen, M.; Wang, X.; Zhao, X.; Wang, Z.; Dang, Z.; Ma, L.; Hu, G.; Chen, F. Triple Shape Memory Effects of Cross-linked Polyethylene/Polypropylene Blends with Cocontinuous Architecture. *ACS Appl. Mater. Interfaces* **2013**, *5*, 5550−5556.
(42) Lützen, H.; Gesing, T. M.; Kim, B. K.; Hartwig, A. Novel Cationically Polymerized Epoxy/Poly(ε-caprolactone) polymers showing a shape memory effect. *Polymer* **2012**, *53*, 6089−6095.
(43) Li, J.; Liu, T.; Xia, S.; Pan, Y.; Zheng, Z.; Ding, X.; Peng, Y. A Versatile Approach to Achieve Quintuple-Shape Memory Effect by Semi-interpenetrating Polymer Networks Containing Broadened Glass Transition and Crystalline Segments. *J. Mater. Chem.* **2011**, *21*, 12213−12217.
(44) Lee, K. M.; Knight, P. T.; Chung, T.; Mather, P. T. Polycaprolactone−POSS Chemical/Physical Double Networks. *Macromolecules* **2008**, *41*, 4730−4738.
(45) Wang, J.; Dong, C. Physical properties, Crystallization Kinetics, And Spherulitic Growth of Well-Defined Poly(ε-caprolactone)s with Different Arms. *Polymer* **2006**, *47*, 3218−3228.